Revue des Composites et des Matériaux Avancés-Journal of Composite and Advanced Materials
Vol. 35, No. 3, June, 2025, pp. 491-496
Journal homepage: http://iieta.org/journals/rcma

Gas Sensor Construction from Cu_3N Thin Films

Mohammed Shareef Mohammed[1*], Seenaa Essa Kadhim[2]

[1] Physics Department, Samarra University, Samara 34010, Iraq
[2] Physics Department, Ministry of Education, Karbala 56001, Iraq

Corresponding Author Email: muhshr@gmail.com

https://doi.org/10.18280/rcma.350310

Received: 3 May 2025
Revised: 5 June 2025
Accepted: 11 June 2025
Available online: 30 June 2025

Keywords:
X-ray, gas sensor, thin films

ABSTRACT

In this study, Cu_3N films were formed on glass substrates at room temperature using Ar + N_2 working gas discharges to generate Cu_3N films on glass substrates at ambient temperature. Cu_3N particles were created using a DC magnetron sputtering technique. A thorough investigation was conducted into the sensitivity of Cu_3N generated in this manner to NO_2 and NH_3 gases at various temperatures. The results show that the synthesized product exhibits high sensitivity and fast response/recovery time at an ambient temperature of 200°C. Furthermore, compared to the comparable particles, the Cu_3N sheets exhibit a greater sensitivity to NO_2 gas. Cu_3N plates have the potential for sensor applications, as demonstrated by this. The best film for sensing the oxidizing gas (NO_2) was copper nitride, which showed that the sensitivity was equal to 37.78% at a temperature of 200°C, and the spray deposition energy was also 0.05 mJ. While for the reducing gas (NH_3), the sensitivity of the copper nitride film was 26.88% at a temperature of 200°C.

1. INTRODUCTION

The sped up course of industrialization has prompted a fast expansion in toxin discharges and bothered ecological contamination. Powerful techniques should be created to tidy up contamination and safeguard the climate [1]. Recognizes risky gases, including carbon monoxide (CO), oxygen oxides (NOx), ozone and sulfur dioxide (SO_2). Carbon monoxide. Outside it causes air contamination, while inside breathed in huge amounts is extremely hazardous to human wellbeing and causes tipsiness [2]. Among the risky gases, nitrogen nitride might be the most unsafe to the human body. Gas sensors are generally used to recognize low convergences of combustible, dangerous or poisonous gases and to screen ecological contamination [3].

Copper nanoparticles (Cu) have gathered significant interest due to their unique properties compared to their larger counterparts. They are known for their antimicrobial and gas sensor application. At the nanoscale, atoms exhibit enhanced properties primarily due to their increased surface area [2]. Cu, in particular, have become one of the most utilized metal nanoparticles in various medical applications. They play a crucial role in applications such as cancer diagnosis and treatment, as well as in biological applications, including the inhibition of bacteria and fungi. These nanoparticles have shown potential in the field of medical diagnostics and therapy, as well as in combating infections [3].

There is little data available in the writings on the addition of progressive metals (TM) in Cu3N (TM,Cu)N, although copper nitride has been generally considered. Cu3N has been proposed as an interesting substrate for various nanoelectronics and nano-gadgets such as twisted cave junctions [4, 5].

Various studies have shown the possibility of obtaining a variety of non-equilibrium microstructures and phase compositions in films prepared by DC magnetron sputtering. In this work, Cu_3N films are experimentally grown by DC magnetron sputtering, and we report the fusion of Cu_3N particles and platelets and their sensitive NO_2 and alkali properties. The results show that the mixed Cu_3N particles and plates have potential in sensor applications for NO_2 gas detection [6].

For films to be sufficiently effective, media with high optical capacity [7] and copper dots [8] are required. To combine thin films with reasonable effectiveness, different techniques have been used: subatomic wave epitaxy [9, 10], core layer affidavit [11], beat laser testimony, reactive DC [12] and mostly used for HF filtering.

2. EXPERIMENTAL DETAILS

A low-pressure gas discharge device known as a magnetron sputtering system was employed for this project. A stainless steel anode disk for deposited glass substrates, a copper target (cathode), and an evacuated chamber are all included. In front of the cathode was the anode, which generates the electric field necessary for the gas discharge. Using the predetermined conditions of 660V, 8×10^{-2}mbar of chamber pressure, and the associated 3 kV DC power supply. Because it does not react

with the target material, argon gas is frequently used in sputtering processes to create thin films. The reactant and the substance combine to form compounds when a gas, like oxygen , reacts with the target substance is added. When sputtering Cu thin films, using the mixture ratios of Ar +O_2. The most important advantages of the plasma magnetron sputtering are the purity of the deposited material, as well as the adhesion to the surface of the thin films and the Thin films were prepared under vacuum pressure 8×10^{-2}mbar. The optimum conditions through which the thin films of the gas sensor were prepared were under voltage 660V, pressure 8×10^{-2}mbar and current 40mA, as shown in Table 1.

Table 1. Optimal conditions for preparing Cu_3N thin films

Conditions	Values
Working Pressure	8.2×10^{-2}mbar
Discharge Voltage	660V
Discharge Current	40mA
Inter-Electrodes Spacing	5cm
Flow Rate of Ar/N_2	30/70 sccm
Sputtering Time	120 minute

3. SUBSTRATE PREPARATION

Microscope plates used are made of borosilicate glass with dimensions of 25.4 mm × 76.2 mm × 1.0 mm and they were prepared by Barcopharma, China. The substrates are strictly cleaned up before being coated with the film.

Step 1 is achievable by using running water to allow rinsing of any contaminant of planktons that occur naturally in the environment. Contact with commercial cleaning agents must be avoided with even the last chemicals interfering with the adhesion and the same is likely to cause surface scratches which are defective in consequent uniformity.

Step 2 is ultrapure water immersion and the washing with an ultrasonic irradiation during 15 min.

Step 3 reports that the transfer of the substrates is done on the layer of 99% ethanol, which is then subjected to the 30 min of the ultrasonic treatment to deanchor the persistent biocontaminants that are still on the surface.

In Step 4, special drying paper is used to make sure that the volatiles are removed before the particulate falls on the quartz substrates.

On the whole, the methodology described offers a reliable substrate surface devoid of contaminants that is good to produce homogeneous thin-film coatings.

4. SENSOR TEST PROCEDURE

The method of test setup utilizes the following:

1. The sensor is properly mounted in the heater once the test chamber is opened. The chamber is then sealed and an aluminum foil sheet constitutes the basic electrical contacts between the pin feed-through and the sensor.
2. Between the two electrodes a bias potential of about 6 volts is applied.
3. The rotary pump is switched on in order to evacuate the testing chamber to a level of about 1 mbar of pressure. The sensor is adjusted to the desired operating temperature by means of a temperature controller. The electrical circuit of the scheme of measuring the gas detection is shown schematically in Figure 1.
4. The rate of flow is controlled by needle valves to air and the tested gas; The volumetric concentration of (1, 2 and 3) percent test gas is added to the air.
5. The current variation is measured with the help of the digital multimeter of type UNI-UT81B connected to the PC.
6. The digital multimeter records the biasing of current flow in air the first time. Next, the NO_2 or NH_3 test gas is also activated and the current does not change much during the next several seconds. The test gas is then switched off in order to note the recuperation time.
7. The measurements described above are repeated in the case of the other concentration of the test gas as shown in Figure 1.

Additionally, Figure 2 illustrates the optimal condition for sputtering Cu_3N, which is crucial for achieving the desired film properties.

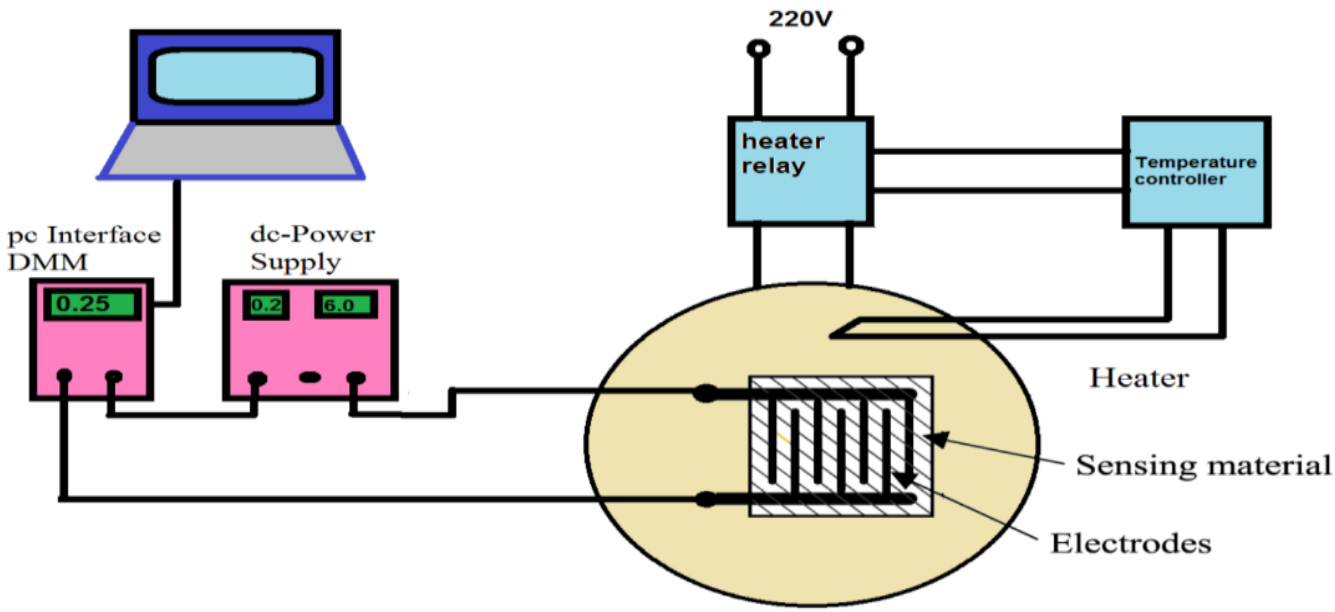

Figure 1. Schematic diagram of gas sensing and the electrical circuit setup [13]

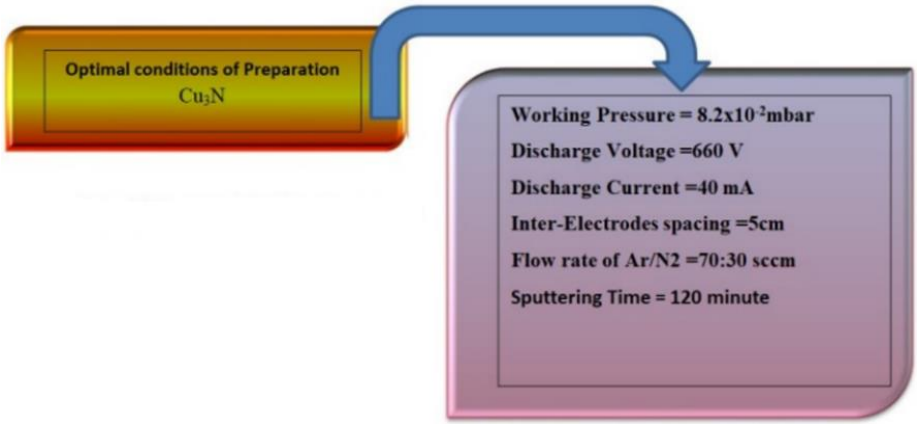

Figure 2. The optimal condition for sputtering Cu_3N

4.1 Results

The X-beam defraction of damaged Cu_3N in the weak films is shown in Figure 3. Such movies had been 1. grown in pure $Ar(70)/N_2(30)$ and pure $Ar(50)/N_2(50)$ gas mixtures, respectively, at room temperature on glass substrates by the thermal decomposition of organometallic precursors. The nanocrystalline nature of the produced material is also confirmed by the diffraction pattern, the occurrence of which at the commensurate angle between the monoclinic lattice parameter of nanoparticles Cu3N. The crystallite dimensions calculated by the Debye-Scherrer equation (D = 0.9)/lambda/theta cos0, where lambda is the wavelength of the X-rays, beta is the full width at half maximum (FWHM) in radians and theta is the Bragg diffraction angle, are 9.5-17.9 nm. The reference [14] shows the XRD pattern of a perfectly pure sample of copper in question of the best quality.The films produced at various gas mixture ratios (Ar/N_2) have a prominent (200) in their XRD spectra. Orientation. The films exhibit a preference for the (100) orientation, as indicated by the XRD spectra. However, the (200) peak becomes more pronounced for varying gas mixtures (Ar/N_2). The mobility of the Cu and N atoms involved in the film growth process is thought to be the primary determinant of the preferred orientation of the as-deposited copper nitride films. It is anticipated that this mobility will depend on both the kinetic energy of the N and Cu atoms as well as the ratio of their numbers that reach the substrate [15], as shown in Table 2.

Table 2. X-ray diffraction characteristics of Cu_3N thin films on glass substrates at various Ar/N_2 gas mixture ratios

Gas (Ar/N_2)	2θ (Deg.)	FWHM (Deg.)	dhkl Exp.(Å)	C.S (nm)	dhkl Std.(Å)	hkl
	35.1278	0.6600	2.5526	12.6	5.7720	(200)
(50/50)	21.6383	0.6400	4.1037	12.6	4.3830	(001)
	24.4521	0.4000	3.6375	20.3	2.7685	(011)
(70/30)	34.8430	0.6700	2.5728	12.4	5.7720	(200)
	38.0753	0.8800	2.3615	9.5	4.3830	(001)
	21.9077	0.4520	0.5400	17.9	4.3830	(001)

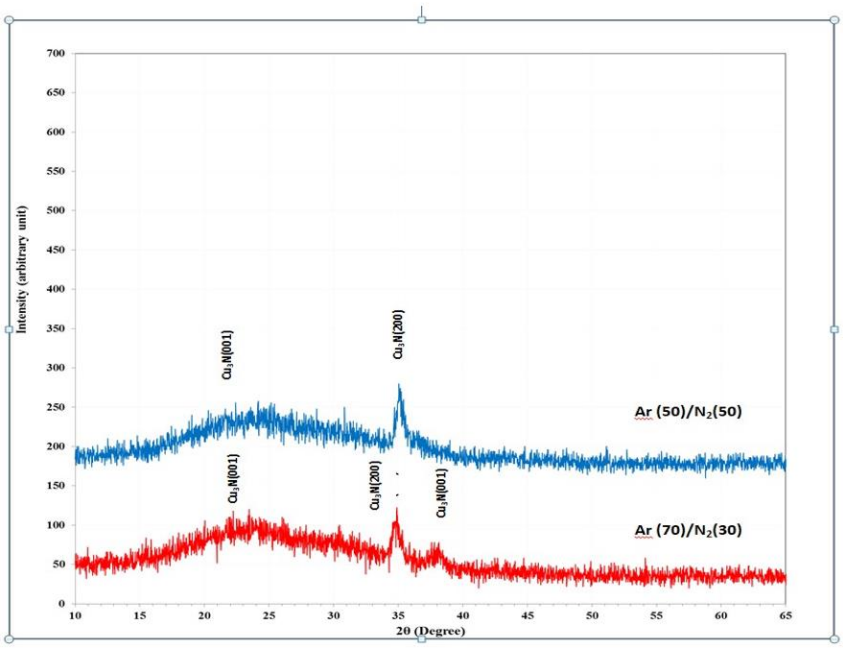

Figure 3. The XRD pattern of Cu_3N nanoparticles at various ratios of the gas mixture (Ar/N_2)

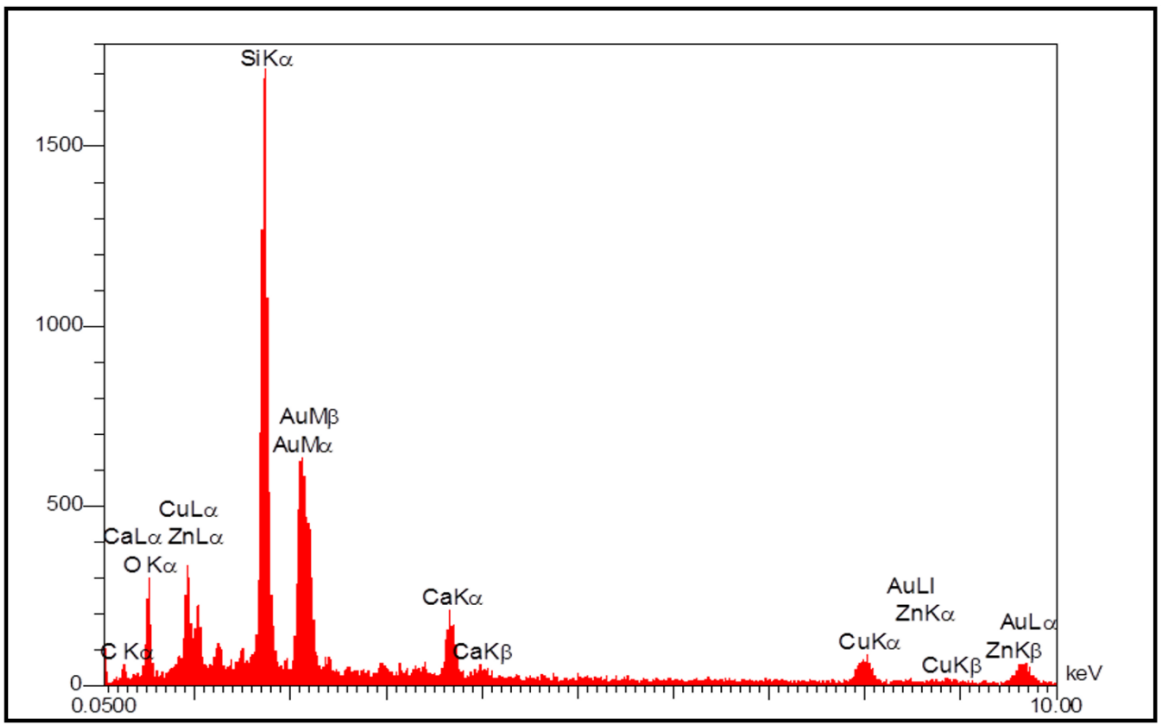

Figure 4. EDX pattern of Cu_3N sample

Therefore, the FE-SEM micrograph shows that the Cu have sizes ranging from 9-12 nm. The average diameters of the copper nanoclusters increase from 190 to 250 nm. From the FE-SEM results, it was found that the particles consist largely of nano-sized particles and some small particles instead of micron-sized particles. This is because the force of DC forms very small nano-sized particles [16, 17], as shown in Figures 4 and 5, the agglomeration of particles with high surface roughness of the copper.

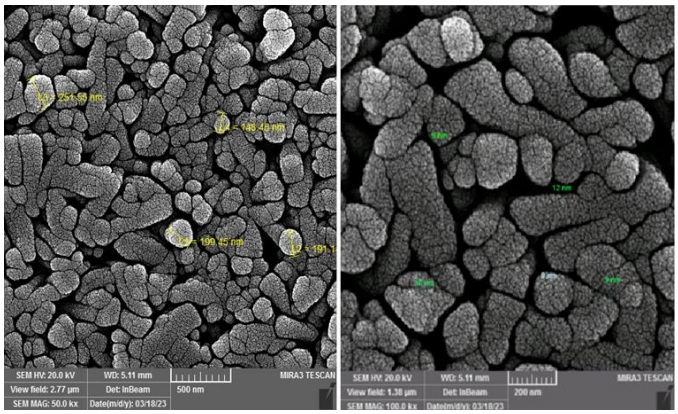

Figure 5. FE-SEM images depicting the surface morphology of Cu_3N

4.2 Measurement of NH_3 gas and measurement of NO_2 gas

In a Cu_3N-based sensor, gas detection is controlled by the surface. The surface response between Cu_3N and gas molecules is crucial for comprehending the gas-sensing mechanisms. As chemisorbed oxygen is added to the surface, its type and amount determine the resistance. Nevertheless, the reaction mechanism for NO_2 is highly complex and involves several intermediate steps. One can explore the optimal operating temperatures for each sample to determine their gas-sensing properties. As shown in Figures 6, 7 and 8, Cu_3N samples react with NO_2. These measurements were conducted at an operating temperature 200°C. All prepared models with resistance variance are shown in Figures 6 and 7 [18, 19].

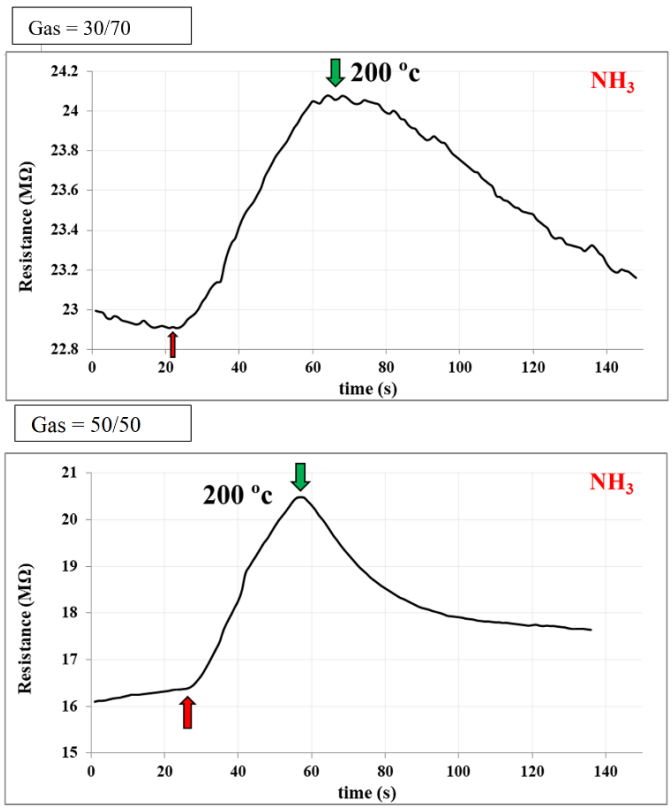

Figure 6. Ammonia gas sensitivity assessment of Cu_3N gas sensors across various Ar/N_2 mixture ratios

The illustrations above demonstrate that the resistivity of a metal oxide semiconductor thin film rises upon the introduction of a gas and falls upon its removal. This behavior can be attributed to the following process: The Cu_3N sensing

mechanism involves the adsorption of gaseous molecules on the surface, resulting in electron transfer between the surface and the gas molecules, which alters the electrical conductivity. NH_3, in this context, acts as a reducing agent. When the sensor is exposed to ambient reducing gases, electrons generated during the chemical reaction for adsorbed oxygen ion formation are returned to the conduction band. In a p-type metal oxide semiconductor sensor, this corresponds to electrons moving into the valence band where they recombine with holes, thereby decreasing the carrier concentration (holes) and lowering the sensor's resistance (leading to increased electrical conductivity). Figure 6 illustrates the models that account for the observed changes in resistance [20, 21].

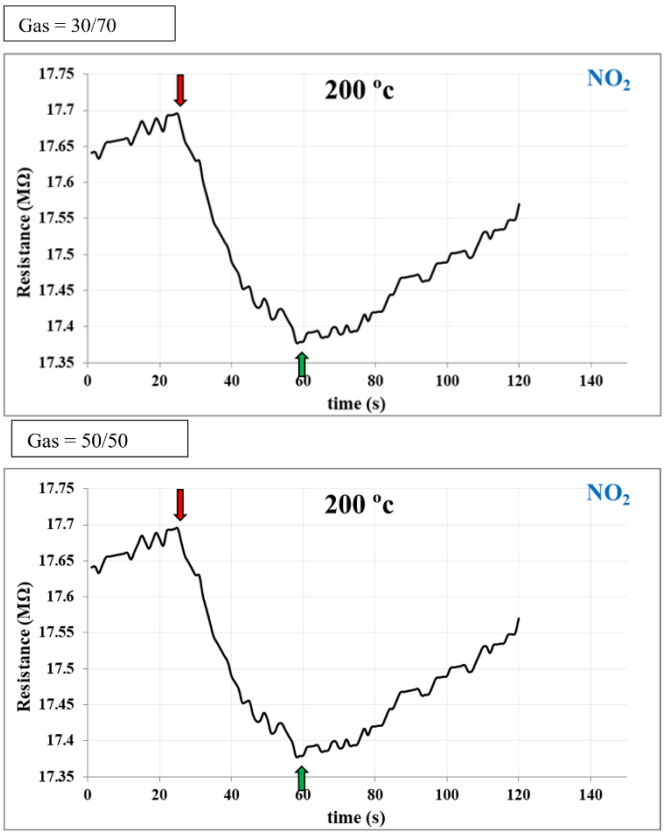

Figure 7. Gas sensor measurements for Cu_3N using NH_3 gas at a different gas mixture ratio (Ar/N_2)

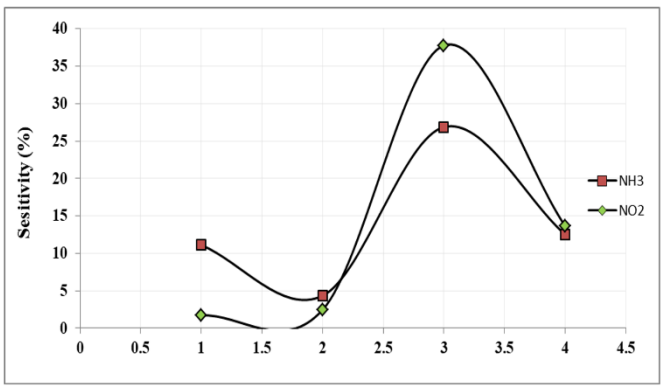

Figure 8. Variation of sensitivity for NO_2 prepared and NH_3 gas for Cu_3N samples at a different gas mixture ratio

The origin of these findings lies in the fact that the resistance levels rise with time of exposure to the gas and drop in time of exposure to our gas: the target gas reacts with the surface of metal oxide film by use of oxygen ions which are absorbed to the surface changing the concentration of charge carriers in the material. The given shift of carrier density affects the conductivity (or resistivity) of the material, as it is depicted in Table 3. Depending on the oxidizing gas used an increase or decrease in conductivity of a P-type semiconductor occurs when NO_2 gas (an oxidizing gas) is applied to it. This is due to the fact that the oxygen ion can extract electrons out of the metal oxide that increases conductivity in the semiconductor. The results in Figure 7 shows that during reaction between an oxidizing gas and an oxidizing semiconductor the resistance decreases as the oxygen ion captures electrons on the surface to create more holes inside the semiconductor. When a p-type metal oxide semiconductor is therefore exposed to NO, the semiconductor will be boosted in its conductance. Figure 8 [22, 23] lists all de-facto models and the respective variation of the resistances.

Table 3. Gas sensor parameters for Cu_3N thin films at different operating temperature against NH_3 and NO_2 gas

Gas Type	Gas Ratio (%)	Sensitivity (%)	Response Time (s)	Recover Time (s)
NH_3	30/70	26.88	30	40
	50/50	12.50	37	50
NO_2	30/70	37.78	27	60
	50/50	13.64	38	52

5. CONCLUSIONS

The capacity of Cu_3N particles and plates to recognize NO_2 and NH_3 was deliberately researched. The outcomes showed that Cu_3N behaved as a p-type semiconductor when prepared. It was discovered that 200°C per plate was the ideal operating temperature for Cu_3N plates to detect NO_2. Compared to Cu_3N particles, Cu_3N plates had a better affectability. This analysis suggested that due to their excellent detecting capabilities and low working temperature, Cu_3N plates could be used to detect NO_2 with little effort and little energy. If a mixture of Argon and Oxygen gases is used, the response will be higher for the gas sensor. The test FESEM is one of the most important structural tests for the prepared thin films, on the basis of which it is chosen whether the surface of the membrane is suitable for testing it as a gas sensor or not.

REFERENCES

[1] Huang, J., Shen, J., Li, S., Cai, J., Wang, S., Lu, Y., Lai, Y. (2020). TiO_2 nanotube arrays decorated with Au and Bi2S3 nanoparticles for efficient Fe^{3+} ions detection and dye photocatalytic degradation. Journal of Materials Science & Technology, 39: 28-38. https://doi.org/10.1016/j.jmst.2019.04.043

[2] Azad, A.M., Akbar, S.A., Mhaisalkar, S.G., Birkefeld, L.D., Goto, K.S. (1992). Solid-state gas sensors: A review. Journal of the Electrochemical Society, 139(12): 3690. https://doi.org/10.1149/1.2069145

[3] Fine, G.F., Cavanagh, L.M., Afonja, A., Binions, R. (2010). Metal oxide semi-conductor gas sensors in environmental monitoring. Sensors, 10(6): 5469-5502. https://doi.org/10.3390/s100605469

[4] Blank, T.A., Eksperiandova, L.P., Belikov, K.N. (2016). Recent trends of ceramic humidity sensors development:

A review. Sensors and Actuators B: Chemical, 228: 416-442. https://doi.org/10.1016/j.snb.2016.01.015

[5] Kong, J., Franklin, N.R., Zhou, C., Chapline, M.G., Peng, S., Cho, K., Dai, H. (2000). Nanotube molecular wires as chemical sensors. Science, 287(5453): 622-625. https://doi.org/10.1126/science.287.5453.622

[6] Zhang, W., de Vasconcelos, E.A., Uchida, H., Katsube, T., Nakatsubo, T., Nishioka, Y. (2000). A study of silicon Schottky diode structures for NOx gas detection. Sensors and Actuators B: Chemical, 65(1-3): 154-156. https://doi.org/10.1016/S0925-4005(99)00466-9

[7] Noh, W., Shin, Y., Kim, J., Lee, W., Hong, K., Akbar, S. A., Park, J. (2002). Effects of NiO addition in WO3-based gas sensors prepared by thick film process. Solid State Ionics, 152-153: 827-832. https://doi.org/10.1016/S0167-2738(02)00341-7

[8] Capone, S., Rella, R., Siciliano, P., Vasanelli, L. (1999). A comparison between V2O5 and WO3 thin films as sensitive elements for NO detection. Thin Solid Films, 350(1-2): 264-268. https://doi.org/10.1016/S0040-6090(99)00045-0

[9] Hamad, A.A., Ahmed, F.M., Kumar, C.L., Donipati, S., Sreekrishna, T., Bandhu, D., Tayyeh, A.M. (2023). Development of cellulose nanocomposites for electromagnetic shielding applications by using dynamic network. Proceedings of the Institution of Mechanical Engineers, Part E: Journal of Process Mechanical Engineering, 09544089231202913. https://doi.org/10.1177/09544089231202913

[10] Patil, L.A., Patil, D.R. (2006). Heterocontact type CuO-modified SnO2 sensor for the detection of a ppm level H2S gas at room temperature. Sensors and Actuators B: Chemical, 120(1): 316-323. https://doi.org/10.1016/j.snb.2006.02.022

[11] Manjula, A., Sangeetha, S., Musa Jaber, M., Hamad Mohamad, A.A., Kumar Sahu, S., Verma, R., Vats, P. (2023). Stratifying transformer defects through modelling and simulation of thermal decomposition of insulating mineral oil. Journal for Control, Measurement, Electronics, Computing and Communications, 64(4): 733-747. https://doi.org/10.1080/00051144.2023.2197821

[12] Eranna, G., Joshi, B.C., Runthala, D.P., Gupta, R.P. (2004). Oxide materials for development of integrated gas sensors—A comprehensive review. Critical Reviews in Solid State and Materials Sciences, 29(3-4): 111-188. https://doi.org/10.1080/10408430490888977

[13] Faris, M.M., Ayal, A.K. (2023). Effect of voltage on gas sensor performance of anodization synthesized TiO_2 nanotubes arrays. Iraqi Journal of Science, 64(12) : 6135-6147. https://doi.org/10.24996/ijs.2023.64.12.5

[14] Fan, X., Wu, Z., Li, H., Geng, B., Li, C., Yan, P. (2007). Morphology and thermal stability of Ti-doped copper nitride films. Journal of Physics D: Applied Physics, 40(11): 3430. https://doi.org/10.1080/10408430490888977

[15] Sen, P., Ghosh, J., Abdullah, A., Kumar, P., Vandana. (2003). Preparation of Cu, Ag, Fe and Al nanoparticles by the exploding wire technique. Journal of Chemical Sciences, 115: 499-508. https://doi.org/10.1007/BF02708241

[16] Hamil, M.I., Khalaf, M.K., AL-Shakban, M. (2022). A study corrosion properties by magnetron sputtered nanocrystalline Al2o3 thin films. Egyptian Journal of Chemistry, 65(11): 413-419. https://doi.org/10.21608/ejchem.2022.123474.5522

[17] Sasidharan, D., Namitha, T.R., Johnson, S.P., Jose, V., Mathew, P. (2020). Synthesis of silver and copper oxide nanoparticles using Myristica fragrans fruit extract: Antimicrobial and catalytic applications. Sustainable Chemistry and Pharmacy, 16: 100255. https://doi.org/10.1016/j.scp.2020.100255

[18] Ahmed, F.M., Mohammed, B.S. (2023). Feasibility of breast cancer detection through a convolutional neural network in mammographs. Tamjeed Journal of Healthcare Engineering and Science Technology, 1(2): 36-43. https://doi.org/10.59785/tjhest.v1i2.24

[19] Pierson, J.F., Horwat, D. (2008). Addition of silver in copper nitride films deposited by reactive magnetron sputtering. Scripta Materialia, 58(7): 568-570. https://doi.org/10.1016/j.scriptamat.2007.11.016

[20] Dighavkar, C.G., Patil, A.V., Patil, S.J., Borse, R.Y. (2009). Ammonia gas sensing performance of Cr2O3-loaded TiO2 thick film resistors. Solid State Science and Technology, 17(2): 197-207.

[21] Karunagaran, B., Uthirakumar, P., Chung, S.J., Velumani, S., Suh, E.K. (2007). TiO2 thin film gas sensor for monitoring ammonia. Materials Characterization, 58(8-9): 680-684. https://doi.org/10.1016/j.matchar.2006.11.007

[22] Kohli, N., Hastir, A., Singh, R. C. (2016). Gas sensing behaviour of Cr_2O_3 and W^{6+}: Cr_2O_3 nanoparticles towards acetone. AIP Conference Proceedings, 1731(1): 050044. https://doi.org/10.1063/1.4947698

[23] Gordon, W.O. (2006). Metal Oxide Nanoparticles: Optical Properties and Interaction with Chemical Warfare Agent Simulants. http://hdl.handle.net/10919/29634.